in the formation of complexes between the polymeric procyanidins and other types of biopolymers. It may also become important in potential commercial applications of these polymers.

Acknowledgment. This research was supported by a grant from the U.S. Department of Agriculture, 87-FSTY-9-0256. We gratefully acknowledge the use of equipment of Professor Michael Rodgers' laboratory at Bowling Green State University.

Registry No. Procyanidin B1, 20315-25-7; procyanidin B2, 29106-49-8; procyanidin B3, 23567-23-9; procyanidin B4, 29106-51-2; procyanidin B5, 12798-57-1; procyanidin A1, 12798-56-0.

Dodecamethoxyorthocyclophane: Conformational and Dynamic Properties Studied by Proton 2D Exchange NMR

A. Maliniak,[†] Z. Luz,*[,†] R. Poupko,[†] C. Krieger,[‡] and H. Zimmermann[‡]

Contribution from The Weizmann Institute of Science, Rehovot 76100, Israel, and Max-Planck-Institut für Medizinische Forschung, Postfach 103820, D-6900 Heidelberg, West Germany. *Received November 1, 1989*

Abstract: A new member of the orthocyclophane series, i.e., 3,4,5,10,11,12,17,18,19,24,25,26-dodecamethoxy[1.1.1.1]-orthocyclophane (DCP), has been synthesized and its conformational and dynamic properties studied by 1D and 2D proton NMR spectroscopy. Its proton NMR exhibits in solutions two subspectra due to two conformers. Molecular mechanics calculations and NMR chemical shift data indicate that these conformers correspond to the sofa and boat forms, respectively. The equilibrium constant between the two forms was determined at room temperature in a number of solvents. In all cases the ratio [sofa]/[boat] was larger than unity, but in general this ratio decreased with increasing the polarity of the solvent. Two-dimensional exchange NMR experiments were performed in order to investigate the various rearrangement mechanisms involving the two conformers. The results at 30 °C in a nitrobenzene solution show that the direct sofa–sofa pseudorotation is most rapid (k_1 = 6.8 s^{-1}), while pseudorotation of the boat is slow and proceeds mainly indirectly via the sofa form. There are two distinct sofa–boat interconversion processes with comparable rate constants (k_3 = 4.5 and k_4 = 4.7 s^{-1}). X-ray diffraction measurements indicate that DCP crystals are monoclinic and belong to the space group $P2_1/a$. There are two symmetry-related molecules per unit cell located at points of inversion symmetry, with geometry corresponding to that of the sofa conformation.

I. Introduction

Several new derivatives of the cycloveratrylene series (**1**) have recently been prepared in connection with a study of the mesomorphic properties of macrocyclic compounds.[1-8] So far only cycloveratrylenes with n = 2, 3, and 4 have been isolated and definitively identified.[9] It is likely that higher homologues have also been formed during the synthesis of the lower homologues, but up to now they have not been isolated.[8] The molecules of the n = 2 and 4 members of the series were shown by NMR to be highly flexible and to undergo, respectively, fast ring inversion[10] and pseudorotation.[9] In contrast the n = 3 homologue has a rigid structure with C_{3v} symmetry, which undergoes extremely slow ring inversion even at 200 °C.[11,12]

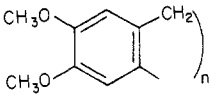

1

Two stable conformations of the cyclotetraveratrylene homologue have been considered, the "sofa" (2A) with C_{2h} symmetry and the "boat" (2B) with C_{2v} symmetry. The more symmetric "crown" (2C) conformer (with C_{4v} symmetry) is unstable, apparently due to steric interactions between the aromatic rings.[9] In a dynamic NMR investigation of cyclotetraveratrylene in chloroform solutions White and Gesner[9] observed only one species which they identified with the sofa conformer. They indicated, however, that the fast pseudorotation of this conformation probably proceeds via the boat (or crown) form, although no peaks due to the latter were observed in the ^1H NMR spectrum even at low temperatures where the process is very slow. In preliminary ^1H NMR experiments that we have performed on solutions of cyclotetraveratrylene (octamethoxyorthocyclophane, OCP) in the much more polar solvent, acetonitrile, we have observed similar dynamic effects as did White and Gesner in chloroform. However on cooling to below −40 °C, freezing out of the pseudorotation process occurred and the spectrum exhibited, besides those of the sofa, additional peaks which we identify with the boat conformation of cyclotetraveratrylene. These peaks broaden at the same temperature as those of the sofa and eventually merge with the latter to give a single average spectrum at high temperatures.

In the present paper we extend the above conformational and dynamic studies of the cyclotetraveratrylene to a more highly substituted derivative, i.e., 3,4,5,10,11,12,17,18,19,24,25,26-dodecamethoxy[1.1.1.1]orthocyclophane (DCP) (or, according to our previous nomenclature,[3] 1,2,3,5,6,7,9,10,11,13,14,15-dodecamethoxytetrabenzo[*adgj*]cyclododecatetraene). We find from the NMR spectra at low and room temperatures that in this derivative the stability of the sofa and boat conformations are very nearly equal. At higher temperatures, fast rearrangement, involving pseudorotation and interconversion of the sofa and boat conformations, takes place, which eventually leads to a single average spectrum.

[†] The Weizmann Institute of Science.
[‡] Max-Planck-Institut für Medizinische Forschung.

(1) Zimmermann, H.; Poupko, R.; Luz, Z.; Billard, J. *Z. Naturforsch.* **1985**, *40a*, 149.
(2) Zimmermann, H.; Poupko, R.; Luz, Z.; Billard, J. *Z. Naturforsch.* **1986**, *41a*, 1137.
(3) Poupko, R.; Luz, Z.; Spielberg, N.; Zimmermann, H. *J. Am. Chem. Soc.* **1989**, *111*, 6094.
(4) Zimmermann, H.; Poupko, R.; Luz, Z.; Billard, J. *Liq. Cryst.* **1989**, *6*, 151.
(5) Kranig, W.; Spiess, H. W.; Zimmermann, H. *Liq. Cryst.* **1990**, *7*, 123.
(6) Malthete, J.; Collet, A. *Nouv. J. Chim.* **1985**, *9*, 151.
(7) Levelut, A. M.; Malthete, J.; Collet, A. *J. Physique* **1986**, *47*, 357.
(8) Collet, A. *Tetrahedron* **1987**, *43*, 5725.
(9) White, J. D.; Gesner, B. D. *Tetrahedron* **1974**, *30*, 2273.
(10) Rabideau, P. N. *J. Org. Chem.* **1971**, *36*, 2723.
(11) Miller, B.; Gesner, B. D. *Tetrahedron Lett.* **1965**, 3351.
(12) Collet, A.; Gabard, J. *J. Org. Chem.* **1980**, *45*, 5400.

0002-7863/90/1512-4277$02.50/0

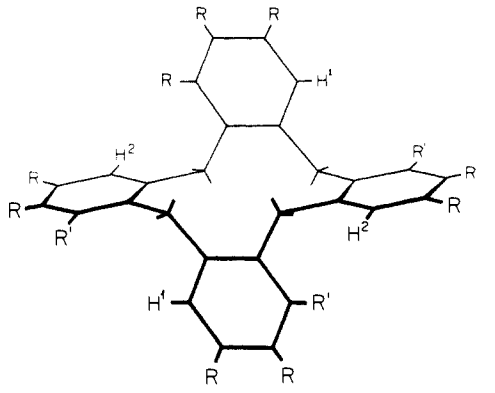

2A

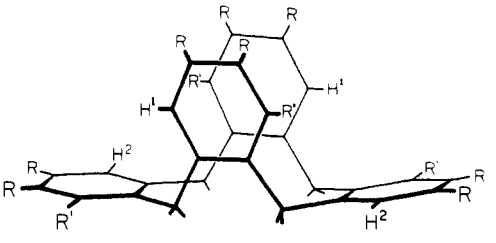

2B

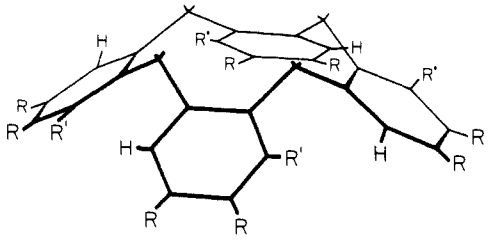

2C

CORE: R = R′ = H
OCP: R = OCH_3; R′ = H
DCP: R = R′ = OCH_3

In section II we briefly describe the synthesis of DCP and other experimental aspects of the work. Then, in section III, we show, by using molecular mechanics calculations on isolated molecules, that indeed the sofa and boat conformations of DCP correspond to energy minima much lower than any other conformation, and we calculate their equilibrium structures. From these results, with use of ring current calculations, the NMR chemical shifts between the various aromatic protons are estimated and used to assign the corresponding experimental peaks of both conformers in the solutions studied. In section IV we present results of molecular structure determination obtained by X-ray diffraction experiments on single crystals of DCP and compare the results with those of the molecular mechanics calculations. Finally, in section IV we use 2D exchange NMR to determine the mechanism and to estimate the kinetic parameters of the various rearrangement processes of DCP in solutions.

The method of 2D exchange spectroscopy introduced, about 10 years ago,[13] has been successfully demonstrated on several $I = 1/2$ systems in isotropic liquids[14-16] and more recently also on $I = 1$ nuclei in liquid crystals.[17,18] In the present work the 2D exchange method turned out to be essential for the elucidation of the rearrangement processes, although the analogous 1D method of saturation transfer could in principle also be used. The 2D exchange method allowed us however to do so in a compact way and to present a self-consistent picture of the various kinetic pathways.

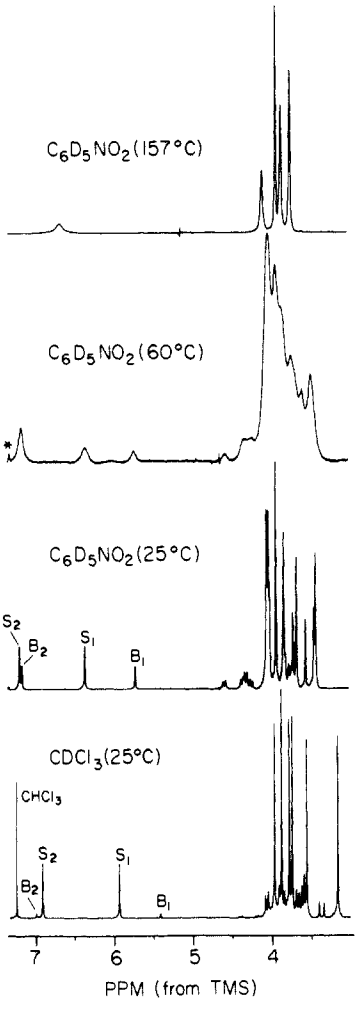

Figure 1. ^1H spectra of DCP in chloroform-*d* and in nitrobenzene-d_5 at the indicated temperatures.

II. Experimental Section

DCP was synthesized following the procedure used previously for OCP.[9] A solution of 3,4,5-trimethoxybenzyl alcohol (Lancaster Synthesis, 5 g) in glacial acetic acid (30 mL) containing 0.5 mL of concentrated H_2SO_4 was continuously stirred at 100 °C for 1 h resulting in a green flocculent precipitate. After allowing to cool the mixture was poured over ice and stirred for another hour, and the green precipitate (2.8 g) was isolated by filtration. Repeated crystallization from ethanol yielded 250 mg of DCP as fine white needle-like crystals (mp 297 °C). A large peak corresponding to $m/z = 720$, as expected for $C_{40}H_{48}O_{12}$, was observed in the mass spectrum, accompanied with weaker peaks at 721, 722, and 723 due to isotopic species. No peaks corresponding to higher molecular weights were observed. Further identification of the product as 3,4,5,10,11,12,17,18,19,24,25,26-dodecamethoxy[1.1.1.1]-orthocyclophane came from ^1H NMR and X-ray diffraction experiments to be described below.

From the mother liquor, after standing for a week at room temperature, a second product was isolated (850 mg) by precipitation and repeated crystallization from ethanol. By using mass spectrometry ($m/z = 540$) and ^1H NMR this product was identified as nonamethoxytribenzocyclononene.[19]

Samples of DCP for the NMR measurements were prepared in various commercially available deuterated solvents, which were used without further treatment. Depending on the solvent the concentrations ranged between 0.1 and 0.4 wt %. The NMR measurements were performed

(13) Jeener, J.; Meier, B. H.; Bachmann, P.; Ernst, R. R. *J. Chem. Phys.* **1979**, *71*, 4546.
(14) Huang, Y.; Macura, S.; Ernst, R. R. *J. Am. Chem. Soc.* **1981**, *103*, 5327.
(15) Meier, B. H.; Ernst, R. R. *J. Am. Chem. Soc.* **1979**, *101*, 6441.
(16) Perrin, C. L.; Gipe, R. K. *J. Am. Chem. Soc.* **1984**, *106*, 4036.
(17) Boeffel, C.; Luz, Z.; Poupko, R.; Vega, A. J. *Israel J. Chem.* **1988**, *28*, 283.
(18) Boeffel, C.; Luz, Z.; Poupko, R.; Zimmermann, H. *J. Magn. Reson.* **1989**, *85*, 329.
(19) Bosch, J.; Canals, J.; Granados, R. *Anales Quimica* **1976**, *72*, 709.

Table I. Chemical Shifts (in ppm) and Spin–Spin Coupling (in Hz) for the Two Subspectra Observed for DCP in Nitrobenzene-d_5 at 25 °C

	aromatic		methoxy						methylene	
sofa	7.20	6.36	4.05	4.03	3.93	3.83	3.67	3.43	$\delta_A = 4.31$, $\delta_B = 3.83$, $J_{AB} = 16.7$	$\delta_A = 3.70$, $\delta_B = 4.03$, $J_{AB} = 15.0$
boat	7.17	5.72	4.04	4.01	3.93	3.72	3.56	3.45	$\delta_A = 4.59$, $\delta_B = 4.24$, $J_{AB} = 16.4$	$\delta_A = 4.36$, $\delta_B = 3.82$, $J_{AB} = 14.8$

on a Bruker AM 500 high-resolution spectrometer by using either single pulses for the 1D spectra or the sequence $(\pi/2)_x$–t_1–$(\pi/2)_x$–τ_m–$(\pi/2)_x$–t_2 (acquisition) for the 2D exchange spectra.[20] In these experiments 256 FID's with sequential t_1 values consisting of 1024 t_2 points were recorded. Each t_1 FID was repeated with proper phase cycling 16 times with a delay time of 2.8 s. The t_2 dwell time was 179 μs, and the t_1 increments were 385 μs. Magnitude mode 2D Fourier transform was performed, after zero filling the t_1 coordinate to 512 points, yielding a sweep width of 2.8 kHz in both dimensions. The $\pi/2$ pulses were 7.5 μs wide, and the mixing time, τ_m, was varied between 0 and 500 ms. The peak intensities were determined by volume integration along both frequency dimensions, and the cross peak intensities are given as averages of the symmetry-related signals.

For the X-ray solid-state measurements several crystals with different morphologies were first examined to ensure the absence of polymorphism. The final measurements were performed on a prismatic crystal of dimensions 0.2 × 0.2 × 0.2 mm, by using an Enraf Nonius CAD4 X-ray diffractometer and employing Mo Kα radiation with a graphite monochromator (λ = 0.7107 Å). In total 3602 reflections were collected up to $\sin\theta/\lambda = 0.62$ Å^{-1} of which 2048 satisfied the criterion $I \geq 3.0\sigma(I)$. The structure was solved by direct methods with MULTAN,[21] and for the refinement full-matrix least-squares fit was applied. For the refinement, isotropical (for H atoms) and anisotropical (for C and O atoms) temperature factors were used until convergence was reached at $R = 0.043$.

III. ^{1}H NMR Spectra and the Molecular Conformation in Solutions

Room-temperature proton NMR spectra of DCP in deuterated chloroform and in deuterated nitrobenzene are depicted in the bottom two traces of Figure 1. The spectra can readily be interpreted in terms of a superposition of two subspectra corresponding to two different DCP conformations of unequal fractional populations. The relative intensities of the two subspectra are about 1:2 in nitrobenzene and about 1:10 in chloroform. In the aromatic region (5.5–7.5 ppm) each subspectrum exhibits two equally intense singlets (of relative intensity, 1), while in the aliphatic region (3.0–4.5 ppm) six distinct singlets (relative intensity, 3) and two AB (or AX) quartets (each with relative intensity, 2) can be identified. The magnetic parameters for the nitrobenzene solution, derived partly by double irradiation experiments, are summarized in Table I. The spectrum of each conformer is consistent with the structural formula of DCP provided we assume that they have a C_2 symmetry axis or a center of inversion. These results are consistent with the identification of the dodecamethoxy isomer as given in the Experimental Section; however, they do not rule out the possibility of the 3,4,5,11,12,13,17,18,19,25,26,27-isomer. Definitive identification of the DCP as the 3,4,5,10,11,12,17,18,19,24,25,26-isomer was obtained from the X-ray results described in the next section.

To determine the most likely conformations we performed an extensive search of minimum energy structures by molecular mechanics calculations using the MM2(85) force field parameters.[22] The molecular mechanics calculations were performed in several consecutive steps. First a large number of cyclododecatetraene (CDT) conformations was generated, followed by energy minimization of each structure. Structures with energies not exceeding 5 kcal/mol relative to the most stable conformation were used for further calculations. Subsequently, benzene rings were added to form orthocyclophane (CORE) and then 8 and 12 methoxy groups, to form, respectively, OCP and DCP. Each step was followed by energy minimization as above. For all compounds the calculations showed that the most stable conformation is the boat form followed closely by the sofa (Table II), while all other minimum-energy conformations lie at least 8 kcal/mol higher. In particular, we note that the crown form (see last column in the table) has an excess energy of over 30 kcal/mol for OCP and does not even correspond to a local minimum in DCP. Analysis of the numerical results shows that the main contribution to this excess energy is the van der Waals repulsion between the aromatic protons on adjacent rings, as suggested earlier by White and Gesner.[9]

Table II. Molecular Mechanics Minimum Energies (in kcal/mol) Relative to Those of the Corresponding Boat Conformations

molecule	sofa	crown
cyclododecatetraene (CDT)	4.2	0.0
orthocyclophane (CORE)	1.9	31.3
octamethoxyorthocyclophane (OCP)	4.1	32.6
dodecamethoxyorthocyclophane (DCP)	2.2	

Table III. Chemical Shift Differences (in ppm) between the Aromatic Protons of DCP[a]

	$\delta_{B_1} - \delta_{B_2}$	$\delta_{S_1} - \delta_{S_2}$	$\delta_{B_1} - \delta_{S_1}$
calcd	1.5	1.1	0.4
exptl ($CDCl_3$)	1.59	0.98	0.53
exptl (nitrobenzene)	1.45	0.84	0.64

[a] For assignment of peaks see Figure 1.

These results suffer from the usual limitations of the molecular mechanics method, in particular, the use of generally optimized (rather than specific) force field parameters, and the difficulties in evaluating the interactions between aromatic rings.[23,24] Furthermore, the calculations were performed on isolated molecules, disregarding the interactions with the solvent. The results should therefore not be considered accurate enough to predict exact equilibrium ratios between conformations; however, they certainly suggest that the two conformations observed in solutions of DCP are indeed the sofa and boat.

We note in Figure 1 that, in the spectra of both conformers, there is a significant shift between the two inequivalent aromatic protons, being about 0.8 ppm for the peaks labeled S and 1.5 ppm for the B's. These large chemical shifts as well as the large differences in the shift between the two conformations is presumably dominated by intramolecular ring current effects. These can be estimated from the molecular geometries, and therefore comparison with the experimentally observed shifts should allow us not only to identify the two subspectra with the sofa and boat conformations but also to assign the aromatic peaks with the particular aromatic rings in each conformer. The estimation of the ring current contributions to the chemical shifts were obtained from the parametrized graphs derived from the modified Johnson and Bovey formula[25,26] with use of the atomic coordinates from the molecular mechanics calculations. The contributions from the different rings were assumed to be additive, and the net results are summarized in Table III. Comparison with the results in the $CDCl_3$ and nitrobenzene solvents allows unequivocal assignment of the aromatic peaks to the sofa (S) and boat (B) conformers as given in the spectra of Figure 1. The results can readily be understood in terms of the structures **2A** and **2B** of the two conformers. It may be seen that both the B_1 and S_1 protons are located in the shielding region of one of the neighboring rings,

(20) Ernst, R. R.; Bodenhausen, G.; Wokaun, A. *Principles of Nuclear Magnetic Resonance in One and Two Dimensions*; Clarendon Press: Oxford, 1987; Chapter 9.
(21) Main, P.; Fiske, S. J.; Hull, S. E.; Lessinger, L.; Germain, G.; Duclercq, J. P.; Woolfson, M. M. MULTAN II, A system of computer programs for the automatic solution of crystal structures from X-ray diffraction data; University of York, England and Louvain, Belgium, 1980.
(22) Allinger, N. L. *J. Am. Chem. Soc.* **1977**, *99*, 8127. Burkert, U.; Allinger, N. L. *Molecular Mechanics*; American Chemical Society: Washington, DC, 1982.
(23) Pettersson, I.; Liljefors, T. *J. Comp. Chem.* **1987**, *8*, 1139.
(24) Allinger, N. L.; Lii, J.-H. *J. Comp. Chem.* **1987**, *8*, 1146.
(25) Johnson, C. E.; Bovey, F. A. *J. Chem. Phys.* **1958**, *29*, 1012.
(26) Farnum, D. G.; Wilcox, C. F. *J. Am. Chem. Soc.* **1967**, *89*, 5379.

Table IV. Room-Temperature Equilibrium Constants, K = [sofa]/[boat] of the DCP Conformers in Different Solvents as Determined by Proton NMR Measurements[a]

solvent	ϵ	K
toluene	2.4	4.5
chloroform	4.8	10.3
nitrobenzene	35.7	2.1
acetonitrile	38.8	2.6
DMSO	47.0	1.7

[a] ϵ is the dielectric constant (taken from ref 27) of the pure solvents.

while the B_2 and S_2 protons experience very little ring current effects due to neighboring rings. The difference between B_1 and S_1 reflects the different relative inclinations of the corresponding rings in the minimum energy structures of the two conformers. The somewhat less satisfactory agreement observed for the nitrobenzene solution is most likely due to specific effects of the nitro groups and ring currents of the solvent on the shifts of the solute.

Further support for the identification of the conformers comes from the solvent effect on the equilibrium constant, K = [sofa]/[boat]. We noted that while the sofa structure has a center of symmetry (point group C_i), the boat conformation has a C_2 symmetry axis but no center of symmetry. Consequently the latter is expected to be polar (with 3.9 D according to the molecular mechanics calculations) and therefore to be stabilized by polar solvents, i.e., by solvents with a high dielectric constant. This expectation is closely borne out by the results in Table IV, where K values as determined by ^{1}H NMR intensity measurements in various solvents are summarized. In general in the more polar solvents like DMSO and acetonitrile a relatively large fraction of DCP is in the boat form, while in the less polar solvents its fractional concentration is very small. The correlation is however not perfect since other factors involving specific solvent–solute interaction probably also affect K.

In principle the assignment of the ^{1}H NMR peaks to the boat and sofa conformers could be confirmed on the basis of their expected different behavior in a chiral environment,[28,29] but our effort to do so failed so far. The boat conformer (**2B**) with C_2 symmetry exists as two enantiomers, which in an achiral environment are necessarily at equal concentrations. Each enantiomer contains pairs of homotopic atoms (e.g., the aromatic H^1,H^1 and H^2,H^2) which are externally enantiotopic to the corresponding pairs in the other enantiomer. Therefore in a chiral solvent or in the presence of a chiral shift reagent the externally enantiotopic nuclei will be diastereotopic and exhibit different chemical shifts. In the chiral environment, however, the two enantiomers are not necessarily isoenergetic, and therefore the doubling of the NMR spectrum will in principle be with a relative intensity different from 1:1. The sofa conformer (**2A**) with C_i symmetry is achiral, but the pairs of the symmetry-related atoms are internally enantiotopic. Consequently in a chiral environment these pairs will become inequivalent and exhibit chemically shifted NMR peaks with however relative intensities of exactly 1:1. Proton NMR measurements on a solution of DCP in acetonitrile containing the shift reagent Eu(tfc)$_3$ showed, as expected, doubling of all peaks both of the sofa and of the boat conformers. The relative intensities of the corresponding subspectra were however within our experimental accuracy essentially equal, thus precluding the use of the above criterion to distinguish between the NMR peaks of the sofa and boat conformers.

IV. Crystal Structure and the Molecular Conformation in the Crystalline State

For the sake of completeness we have also studied the molecular structure and packing of DCP in the crystalline state. Crystals of DCP are monoclinic and belong to the space group $P2_1/a$ (No. 14 of the *International Tables of X-ray Crystallography*): a = 9.106 (3) Å, b = 16.369 (5) Å, c = 12.751 (2) Å, β = 101.89 (1)°, Z = 2, D_x = 1.303 g cm^{-3}, and μ(Mo Kα) = 0.896 cm^{-1}. The two symmetry-related DCP molecules in the unit cell have a sofa conformation with perfect inversion symmetry. A projection of the crystal structure onto the ac plane and the structural formula of DCP as determined from the X-ray results are shown in Figure 2a,b. The bond distances, bond angles, and torsional angles derived from these experiments are summarized in Table V. These results confirm the identification of the title compound as the 3,4,5,10,11,12,17,18,19,24,25,26-isomer of DCP and, in particular, rule out the possibility of 3,4,5,11,12,13,17,18,19,25,26,27-dodecamethoxy[1.1.1.1]orthocyclophane. Comparing the molecular structure derived from the X-ray results with that of sofa conformation obtained from the molecular mechanics calculations shows good agreement for the C–C and C–O bond distances, while the crystallographically determined C–H bond distances are systematically 10–20% shorter. The values of the bond and dihedral angles of the molecular skeleton are also well reproduced by the calculations; however, the positions of the methoxy groups obtained by the two methods differ significantly. In particular the sofa form obtained from molecular mechanics calculations has no inversion symmetry. This difference is most likely due to the fact that in the calculations on the isolated molecule the position of the methoxy groups is determined by a very shallow local rotational potential around the C–O bonds, while in the solid it is determined by the much stronger crystalline packing forces.

Scheme I

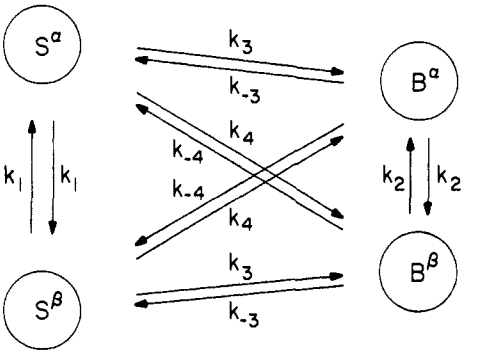

V. The Kinetics of the Conformational Equilibria

Dynamic 1D spectra in nitrobenzene at 60 °C and 157 °C are included in Figure 1. It may be seen that the peaks of both the sofa and the boat conformations start to broaden at about the same temperature, followed by a wide temperature range over which coalescence takes place, resulting finally in a spectrum consisting of a single aromatic peak (of relative integrated intensity 1), a single methylene peak (intensity 2), and three methoxy peaks (each with intensity 3), corresponding to an "average molecule" with C_{4h} symmetry. Clearly several rearrangement processes take place including pseudorotation of the sofa and boat forms as well as interconversion between the two conformations. The most general kinetic scheme describing this situation is described in Scheme I, where the superscript α and β indicate the two forms of the sofa and boat conformers (and should not be confused with the subscript 1 and 2 in Figure 1, which designate the aromatic hydrogens of the corresponding conformers). In this scheme k_1 and k_2 are the first-order rate constants for the direct pseudorotation of the sofa and boat forms, respectively, and k_3 and k_4 are rate constants for two different sofa–boat interconversion processes. Note that $k_{-3}/k_3 = k_{-4}/k_4 = K$. Although, in principle, a full quantitative line shape analysis of the dynamic 1D spectrum could provide all the rate constants involved in this scheme, in practice it did not prove possible, because in the intermediate regime, where the line shapes are most sensitive to the detailed mechanism, the peaks of the aromatic protons are smeared out beyond detection, while in the aliphatic region there is excessive overlap of the methylene

(27) Landolt-Börnstein, Zahlenwerte und Funktionen; Springer: Berlin, 1969; Vol. 6.
(28) Mislow, K.; Raban, M. *Top. Stereochem.* **1967**, *1*, 1.
(29) Eliel, E. L. *J. Chem. Educ.* **1980**, *57*, 52.
(30) Reference deleted in proof.

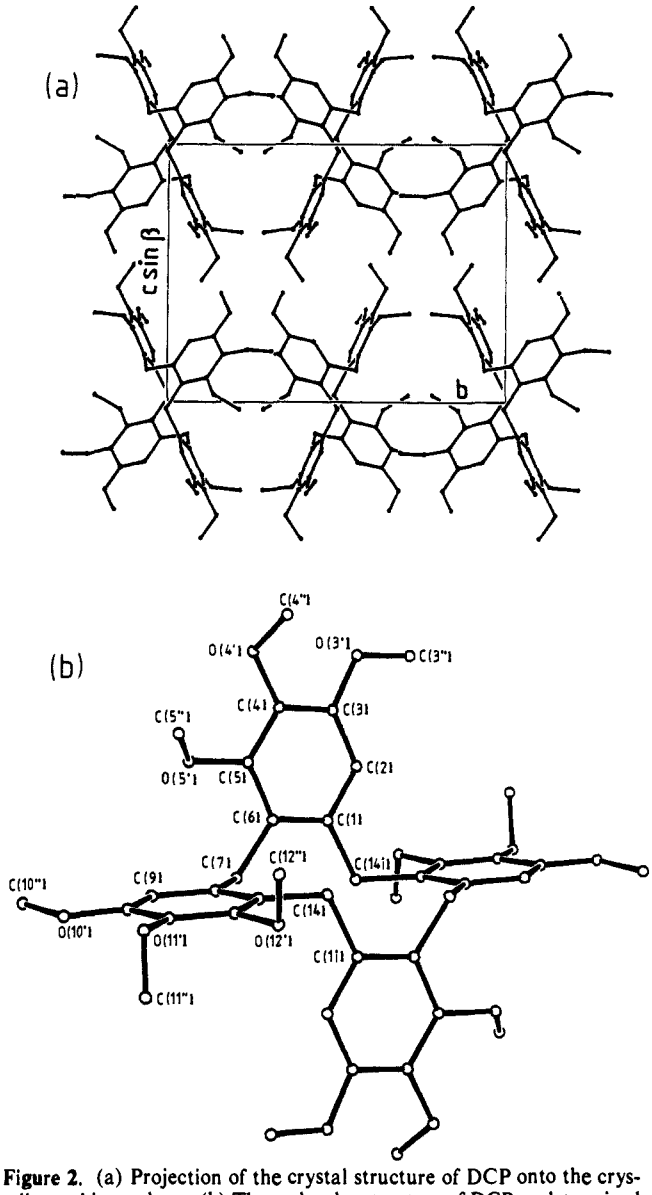

Figure 2. (a) Projection of the crystal structure of DCP onto the crystallographic ac plane. (b) The molecular structure of DCP as determined in the solid state and the atomic numbering system used. The structural parameters are summarized in Table V.

and methoxy protons. Instead, we have therefore performed 2D exchange experiments, limiting the observations to the aromatic protons in the slow exchange regime. Before discussing these experiments, we refer again to the 1D spectra in Figure 1. It can readily be seen, e.g., from the trace at 60 °C, that the width of the sofa peak (S_1) is very similar, or even slightly larger, than that of the boat (B_1), despite the fact that the ratio [sofa]/[boat] is close to 2. This clearly indicates that only part of the broadening is due to sofa–boat interconversion and that at least the sofa–sofa pseudorotation is of comparable rate. These conclusions are borne out by the 2D exchange experiment described below.

The 2D exchange measurements were performed at 30 °C on the same solution of DCP in nitrobenzene as used above for the 1D measurements, and the analysis was confined to the aromatic region of the spectrum. Examples of 2D spectra for three different mixing times, τ_m, are shown in Figure 3, and the integrated intensities of the resulting peaks, or combination of peaks, over the studied range of τ_m are plotted in Figure 4. From the general theory of 2D exchange spectroscopy[31] the dependence of the diagonal (I_{ii}) or cross (I_{is}) peak intensity on τ_m is given by

$$I_{is}(\tau_m) = [\exp(-\tau_m \mathbf{L})]_{is} M_s^0 \qquad (1)$$

(31) Reference deleted in proof.

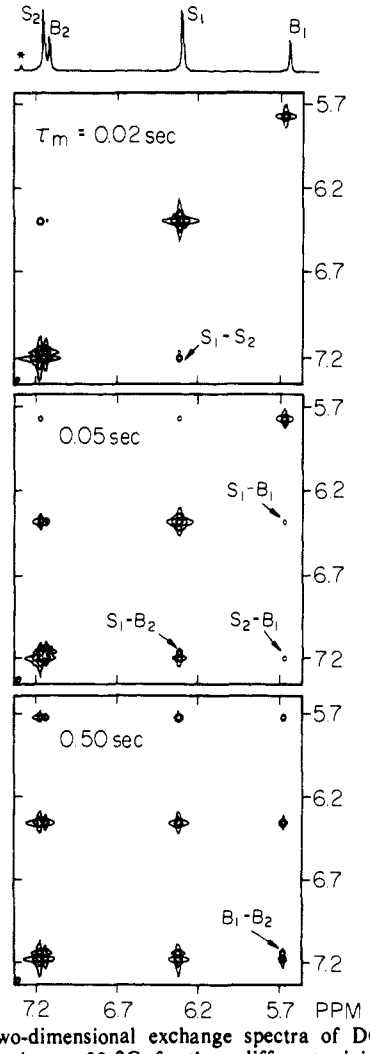

Figure 3. Two-dimensional exchange spectra of DCP in a nitrobenzene-d_5 solution, at 30 °C, for three different mixing times, τ_m, as indicated.

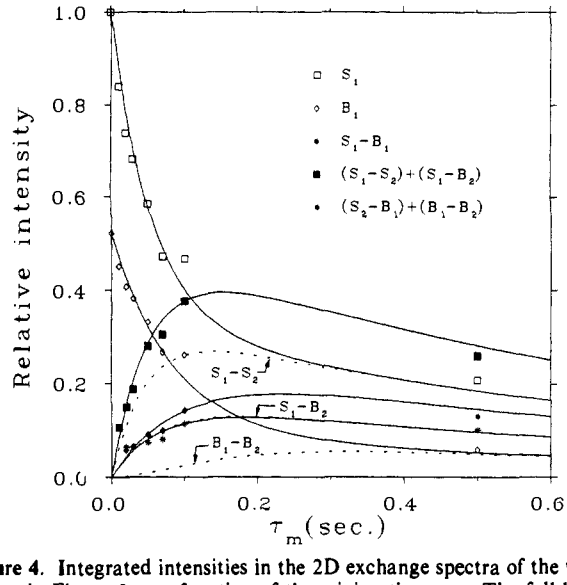

Figure 4. Integrated intensities in the 2D exchange spectra of the type shown in Figure 3 as a function of the mixing time, τ_m. The full lines are for either isolated or pairs of closely spaced peaks, while the dashed lines are for peaks that could not separately be measured in the experiments. The parameters used in the calculations were $1/T_1 = 1.15$, $k_1 = 6.8$, $k_2 = 0$, $k_3 = 4.5$, and $k_4 = 4.7$ s^{-1}. Note that the curves for S_1–B_1 (full) and for S_1–B_2 (dashed) nearly coincide.

where M_s^0 is the equilibrium magnetization of the exchanging peaks (in our case the aromatic signals B_1, S_1, B_2, and S_2), and

Table V. Bond Distances (Å) (a), Bond Angles (deg) (b), and Torsional Angles (deg) (c) for DCP Derived from the X-ray Results[a]

(a) Bond Distances

C(1)–C(2)	1.393 (3)	C(4)–O(4′)	1.375 (3)	C(9)–C(10)	1.373 (3)	C(13)–C(14)	1.510 (3)
C(1)–C(6)	1.394 (3)	C(5)–C(6)	1.394 (3)	C(10)–C(11)	1.390 (3)	O(3′)–C(3″)	1.412 (4)
C(1)–C(14i)	1.519 (3)	C(5)–O(5′)	1.379 (3)	C(10)–O(10′)	1.376 (2)	O(4′)–C(4″)	1.453 (4)
C(2)–C(3)	1.375 (3)	C(6)–C(7)	1.514 (3)	C(11)–C(12)	1.379 (3)	O(5′)–C(5″)	1.425 (4)
C(3)–C(4)	1.386 (3)	C(7)–C(8)	1.521 (3)	C(11)–O(11′)	1.374 (3)	O(10′)–C(10″)	1.424 (3)
C(3)–O(3′)	1.363 (3)	C(8)–C(9)	1.386 (3)	C(12)–C(13)	1.391 (3)	O(11′)–C(11″)	1.420 (4)
C(4)–C(5)	1.383 (3)	C(8)–C(13)	1.390 (3)	C(12)–O(12′)	1.378 (2)	O(12′)–C(12″)	1.430 (4)
C(2)–H(2)	0.968 (20)	C(3″)–H(3A)	0.908 (28)	C(5″)–H(5A)	0.939 (33)	C(11″)–H(11A)	0.815 (30)
C(7)–H(7A)	0.976 (20)	C(3″)–H(3B)	1.035 (34)	C(5″)–H(5B)	0.899 (39)	C(11″)–H(11B)	0.975 (37)
C(7)–H(7B)	0.972 (20)	C(3″)–H(3C)	0.993 (34)	C(5″)–H(5C)	0.984 (35)	C(11″)–H(11C)	0.89 (5)
C(9)–H(9)	0.947 (20)	C(4″)–H(4A)	0.882 (36)	C(10″)–H(10A)	0.996 (25)	C(12″)–H(12A)	0.885 (38)
C(14)–H(14A)	1.006 (22)	C(4″)–H(4B)	0.95 (5)	C(10″)–H(10B)	0.982 (27)	C(12″)–H(12B)	0.95 (5)
C(14)–H(14B)	0.982 (19)	C(4″)–H(4C)	0.970 (44)	C(10″)–H(10C)	1.006 (30)	C(12″)–H(12C)	0.952 (43)

(b) Bond Angles

C(2)–C(1)–C(6)	119.7 (2)	C(1)–C(6)–C(5)	118.2 (2)	C(11)–C(12)–C(13)	122.4 (2)
C(2)–C(1)–C(14i)	118.8 (2)	C(1)–C(6)–C(7)	122.4 (2)	C(11)–C(12)–O(12′)	119.4 (2)
C(6)–C(1)–C(14i)	121.5 (2)	C(5)–C(6)–C(7)	119.4 (2)	C(13)–C(12)–O(12′)	118.2 (2)
C(1)–C(2)–C(3)	121.2 (3)	C(6)–C(7)–C(8)	117.5 (2)	C(8)–C(13)–C(12)	118.1 (2)
C(2)–C(3)–C(4)	119.7 (2)	C(7)–C(8)–C(9)	118.1 (2)	C(8)–C(13)–C(14)	122.3 (2)
C(2)–C(3)–O(3′)	124.8 (2)	C(7)–C(8)–C(13)	122.1 (2)	C(12)–C(13)–C(14)	119.6 (2)
C(4)–C(3)–O(3′)	115.5 (2)	C(9)–C(8)–C(13)	119.8 (2)	C(1i)–C(14)–C(13)	115.1 (2)
C(3)–C(4)–C(5)	119.1 (2)	C(8)–C(9)–C(10)	121.2 (3)	C(3)–O(3′)–C(3″)	117.9 (3)
C(3)–C(4)–O(4′)	121.3 (2)	C(9)–C(10)–C(11)	119.9 (2)	C(4)–O(4′)–C(4″)	113.0 (3)
C(5)–C(4)–O(4′)	119.6 (2)	C(9)–C(10)–O(10′)	124.6 (2)	C(5)–O(5′)–C(5″)	117.1 (3)
C(4)–C(5)–C(6)	122.0 (2)	C(11)–C(10)–O(10′)	115.5 (2)	C(10)–O(10′)–C(10″)	116.4 (2)
C(4)–C(5)–O(5′)	120.9 (2)	C(10)–C(11)–C(12)	118.5 (2)	C(11)–O(11′)–C(11″)	115.0 (3)
C(6)–C(5)–O(5′)	116.9 (2)	C(10)–C(11)–O(11′)	120.1 (2)	C(12)–O(12′)–C(12″)	114.8 (3)
		C(12)–C(11)–O(11′)	121.3 (2)		

(c) Torsional Angles

C(6)–C(1)–C(2)–C(3)	0.7	C(5)–C(4)–O(4′)–C(4″)	117.9	C(9)–C(10)–C(11)–O(11′)	177.6
C(14i)–C(1)–C(2)–C(3)	179.1	C(4)–C(5)–C(6)–C(1)	−1.3	O(10′)–C(10)–C(11)–C(12)	−179.5
C(2)–C(1)–C(6)–C(5)	−0.7	C(4)–C(5)–C(6)–C(7)	−179.8	O(10′)–C(10)–C(11)–O(11′)	−2.1
C(2)–C(1)–C(6)–C(7)	177.7	O(5′)–C(5)–C(6)–C(1)	174.0	C(9)–C(10)–O(10′)–C(10″)	−3.2
C(14i)–C(1)–C(6)–C(5)	−179.0	O(5′)–C(5)–C(6)–C(7)	−4.5	C(11)–C(10)–O(10′)–C(10″)	176.4
C(14i)–C(1)–C(6)–C(7)	−0.7	C(4)–C(5)–O(5′)–C(5″)	−62.9	C(10)–C(11)–C(12)–C(13)	0.1
C(1)–C(2)–C(3)–C(4)	1.3	C(6)–C(5)–O(5′)–C(5″)	121.7	C(10)–C(11)–C(12)–O(12′)	−177.4
C(1)–C(2)–C(3)–O(3′)	−177.0	C(1)–C(6)–C(7)–C(8)	125.0	O(11′)–C(11)–C(12)–C(13)	−177.3
C(2)–C(3)–C(4)–C(5)	−3.2	C(5)–C(6)–C(7)–C(8)	−56.6	O(11′)–C(11)–C(12)–O(12′)	5.2
C(2)–C(3)–C(4)–O(4′)	−179.6	C(6)–C(7)–C(8)–C(9)	120.4	C(10)–C(11)–O(11′)–C(11″)	103.2
O(3′)–C(3)–C(4)–C(5)	175.2	C(6)–C(7)–C(8)–C(13)	−61.1	C(12)–C(11)–O(11′)–C(11″)	−79.4
O(3′)–C(3)–C(4)–O(4′)	−1.2	C(7)–C(8)–C(9)–C(10)	178.6	C(11)–C(12)–C(13)–C(8)	−0.3
C(2)–C(3)–O(3′)–C(3″)	0.3	C(13)–C(8)–C(9)–C(10)	0.2	C(11)–C(12)–C(13)–C(14)	−178.3
C(4)–C(3)–O(3′)–C(3″)	−178.0	C(7)–C(8)–C(13)–C(12)	−178.3	O(12′)–C(12)–C(13)–C(8)	177.3
C(3)–C(4)–C(5)–C(6)	3.3	C(7)–C(8)–C(13)–C(14)	−0.3	O(12′)–C(12)–C(13)–C(14)	−0.7
C(3)–C(4)–C(5)–O(5′)	−171.8	C(9)–C(8)–C(13)–C(12)	0.1	C(11)–C(12)–O(12′)–C(12″)	−69.8
O(4′)–C(4)–C(5)–C(6)	179.7	C(9)–C(8)–C(13)–C(14)	178.1	C(13)–C(12)–O(12′)–C(12″)	112.5
O(4′)–C(4)–C(5)–O(5′)	4.6	C(8)–C(9)–C(10)–C(11)	−0.3	C(8)–C(13)–C(14)–C(1i)	−85.3
C(3)–C(4)–O(4′)–C(4″)	−65.8	C(8)–C(9)–C(10)–O(10′)	179.3	C(12)–C(13)–C(14)–C(1i)	92.7
		C(9)–C(10)–C(11)–C(12)	0.2		

[a] For the numbering system see Figure 2b. Numbers in parentheses are estimated standard deviations in the least significant digits.

L is the exchange (and relaxation) matrix. The chemical kinetic part of this matrix consists of the off-diagonal elements $L_{is} = -k_{si}$, where k_{si} is the first-order rate constant for exchange from site s to i, and the diagonal elements $L_{ii} = \sum_s k_{is}$. For the overall rearrangement scheme described above this matrix becomes

$$\mathbf{L} = \begin{vmatrix} \frac{1}{T_1^{S_1}}+k_2+k_{-3}+k_{-4} & -k_3 & -k_2 & -k_4 \\ -k_{-3} & \frac{1}{T_1^{S_1}}+k_1+k_3+k_4 & -k_{-4} & -k_1 \\ -k_2 & -k_4 & \frac{1}{T_1^{S_2}}+k_2+k_{-3}+k_{-4} & -k_3 \\ -k_{-4} & -k_1 & -k_{-3} & \frac{1}{T_1^{S_2}}+k_1+k_3+k_4 \end{vmatrix} \quad (2)$$

where $1/T_1$ are the longitudinal relaxation rates of the protons in site i, and we have neglected cross relaxation effects because of the large distances (and therefore small dipolar interactions) between the various aromatic protons in the DCP molecule. Expanding eq 1 in powers of τ_m

$$I_{is} = \left[\delta_{is} - L_{is}\tau_m + \frac{1}{2}\sum_k L_{ik}L_{ks}\tau_m^2 - \frac{1}{6}\sum_{l,k} L_{il}L_{lk}L_{ks}\tau_m^3 + \ldots\right]M_s^0 \quad (3)$$

emphasizes the different behavior of direct (first order) and indirect (second or higher orders) exchange processes. In particular it may be seen that for short mixing times the intensity of first-order cross peaks increases linearly with τ_m, while cross peaks corresponding to higher order exchange processes increase as τ_m^2, τ_m^3, etc.

Referring to the 2D diagram (Figure 3) at very short τ_m (0.02 s) it may be seen that only one pair of intense cross peaks connecting the diagonal S_1 and S_2 signals are observed, confirming the earlier conclusion from the 1D spectra that direct pseudorotation is indeed a significant contribution to the overall first-order rate of the sofa form. Next to appear (see diagram for $\tau_m = 0.05$ s) are the two pairs of cross peaks connecting the diagonal sofa and boat signals, S_1–B_1 and S_2–B_1. From the fact that their intensities are nearly the same, it follows that the two sofa-to-boat interconversion mechanisms must have similar rates. Finally the

last cross peaks to appear are the pair B_1–B_2 (see diagram for τ_m = 0.50 s), indicating that if the boat form can undergo direct pseudorotation at all, it must be much slower than the corresponding process in the sofa. In connection with these results two comments must be made. One relates to the fact that the S_1–B_2 peaks, which by symmetry must have the same intensity as the pair S_2–B_1, seem to appear already at τ_m = 0.02 s. It may be seen, however, that this is due to the proximity effect of the more intense S_1–S_2 signals. Likewise the S_2–B_2 cross peaks are obscured due to their proximity to the corresponding, much stronger diagonal signals.

To determine the rate constants of the various rearrangement processes in DCP we performed a least-squares fit analysis (GENLSS[32]) of the observed τ_m dependence of the diagonal and off-diagonal peak intensities (Figure 4) to the parameters of eq 1. The relative equilibrium magnetizations, $K = M^0_{S_1}/M^0_{B_1}$, was estimated from a 2D exchange experiment with $\tau_m = 0$, giving K = 1.9. This value is very close to K = 2.1 determined from the 1D spectrum at 30 °C. Preliminary analysis of separate traces from the 2D spectra indicated that the rate constant for the direct boat pseudorotation (k_2) is at most 20–25% of that of the pseudorotation of the sofa form (k_1) and most likely much smaller. We have therefore (somewhat arbitrarily) set $k_2 = 0$ and fitted the experimental results of Figure 4 to the four parameters, k_1, k_3, k_4, and $1/T_1$ (where we have taken a common longitudinal relaxation rate for all four peaks). Because of the overlap between some of the peaks, we have used in this analysis the intensities of the diagonal S_1 and B_1 signals, the cross peaks S_1–B_1, and the combined peak intensities (S_2–B_1) + (B_1–B_2) and (S_1–S_2) + (S_1–B_2). The cluster corresponding to S_2, B_2 and the two S_2–B_2 cross peaks was not included in the calculations. The final results of this analysis gave $k_2 = 0$, $k_1 = 6.8$, $k_3 = 4.5$, $k_4 = 4.7$, and $1/T_1$ = 1.15 s^{-1}. The value obtained for $1/T_1$ is consistent with that measured by an independent inversion recovery experiment (taking in the analysis proper account of the kinetics processes[33]). The various curves in Figure 4 were calculated by using these least-squares fit parameters. Considering the large uncertainties in the intensity measurements the fit seems quite satisfactory and confirms the preliminary estimation that the dominant rearrangement processes are the sofa pseudorotation and the sofa–boat interconversion. The actual values of the k's must however be considered as tentative and not better than ±30%. Within this uncertainty limit, the results are in agreement with the dynamic line broadening observed in the 1D spectra in the slow exchange regime. Thus at 30 °C the observed line widths of the aromatic sofa and boat peaks in the nitrobenzene solution are $1/T_2^S$ = 19.7 and $1/T_2^B$ = 16.1 s^{-1}. The broadening due to the chemical exchange can be predicted from the rates determined in the 2D experiments

$$\left(\frac{1}{T_2^S}\right)_{ex} = k_1 + k_3 + k_4 = 16.0\ s^{-1} \qquad (4a)$$

$$\left(\frac{1}{T_2^B}\right)_{ex} = k_2 + k_{-3} + k_{-4} = 17.5\ s^{-1} \qquad (4b)$$

Allowing for an exchange independent contribution (including the field inhomogeneity) of about 3–4 s^{-1} yields predicted 1D line widths of 20 and 21 s^{-1}, respectively, in reasonable agreement with the experimental $1/T_2^S$ and $1/T_2^B$.

We finally mentioned that from line width measurements in the 1D spectra at different temperatures, an average activation energy (over the various dynamic processes) of 12.0 and 11.0 kcal/mol have been estimated for the sofa and boat species, respectively. These results are comparable to that of White and Gesner[9] (10.9 kcal/mol) determined for the pseudorotation of OCP in chloroform.

VI. Summary and Conclusions

We have shown by high-resolution ^1H NMR that dodecamethoxy- (and in fact also octamethoxy-)orthocyclophane exists in solution in two interconverting conformations, which on the basis of molecular mechanics calculations and chemical shift data are identified as the sofa and boat forms **2A** and **2B**. Their equilibrium concentrations were found to depend on the solvent polarity with the latter conformer being stabilized by more polar solvents. Two-dimensional exchange experiments allowed us to elucidate the dominant rearrangement processes in solutions of DCP. These are the sofa–sofa pseudorotation and sofa–boat interconversion. As conjectured many years ago by White and Gesner[9] the boat conformer is much less flexible and mainly pseudorotates indirectly via a sofa intermediate although a slow direct pseudorotation cannot be ruled out completely by the experiments. Apparently the direct mechanism must proceed via the crown form which as shown by the molecular mechanics calculations has very high energy and therefore is a very unlikely intermediate. Somewhat unexpectedly it is found that k_3 and k_4 are very nearly equal. To better understand these results it would be useful to extend the molecular mechanics calculations to study transition states and the various possible reaction pathways between the thermodynamically stable conformers.

As mentioned in the introduction our interest in orthocyclophane stemmed from the observation that long-chain octa-substituted derivatives of this compound yield mesogens which exhibit columnar mesophases. It is difficult to imagine such structures formed from the boat-shaped molecules because they cannot readily be stacked into columns. For such stacking the sofa and particularly the crown conformation seems more natural. Since the conformation of DCP was found to be sofa in the solid, it is probably like that also in the mesomorphic state. It would be interesting to pursue the study of this point further by direct measurements of cyclophane mesophases, perhaps by deuterium NMR of specifically substituted molecules.

Acknowledgment. This research was partly supported by a grant from G.I.F., the German-Israeli Foundation for Scientific Research and Development, and by the U.S.–Israel, Binational Science Foundation, Jerusalem. One of us (A.M.) is a recipient of a Stone Postdoctoral Fellowship and was also partly supported by the Swedish Institute. We thank Drs. Rodolfo Ghirlando, Robert Glaser, and Hugo Gottlieb for very helpful discussions.

Supplementary Material Available: Tables of positional parameters, temperature factors, bond distances, bond angles, and torsional angles (9 pages); table of observed and calculated structure factors (20 pages). Ordering information is given on any current masthead page.

(32) DeTar, D. F. In *Computer Programs for Chemistry*; Academic Press: New York, 1972; Vol. 4, Chapter 3.
(33) Forsén, S.; Hoffman, R. A. *J. Chem. Phys.* **1964**, *40*, 1189.